CONF-9007149--5

DE91 004407

DEC 0 4 1990

Phase Analysis of Metallic Plutonium-Containing Fuel Alloys Using Neutron Diffraction

M. H. Mueller[a], J. W. Richardson, Jr.[b], R. V. Strain[a] and G. L. Hofman[a]

[a]Fuels and Processes and [b]Intense Pulsed Neutron Source Divisions
Argonne National Laboratory, Argonne, IL 60439

ABSTRACT

Pulsed neutron powder diffraction studies at IPNS have expanded our understanding of the phases present in Integral Fast Reactor (IFR) metal fuel alloys at temperatures in the range of reactor operating conditions. We report results from the binary alloy (U-10wt.%Zr) and ternary alloys (U-8%Pu-10%Zr) and (U-19%Pu-10%Zr). Determining the role and the location of Zr and Pu in these alloys is considered of fundamental importance for maximizing engineering efficiency.

Rietveld profile analysis was utilized to study the phase diagrams. Data were collected at temperatures ranging from 25-650°C. Although the expected U/Pu/Zr phases (α-U, β-U, γ-U, δ-U/Zr/Pu, ζ-U/Pu) were observed in appropriate temperature ranges, there were some unexpected results. Relative amounts of all phases at each temperature were calculated from Rietveld scale factors and inferences were made as to the location of zirconium and plutonium, i.e. amounts in each phase, from site occupancies and absorption characteristics of the phases present. Finally, we were able to identify ZrO and ZrO_{1-x} inclusion phases in the U-Zr alloy present in very small (0.5-1.0%) amounts.

INTRODUCTION

The Integral Fast Reactor (IFR), an advanced reactor concept[1] which has been under development for several years at ANL, is a contender for possible next-generation power reactor use. It makes use of metallic fuel pins which are reprocessed and refabricated in the Fuel Cycle facility - an integral part of the reactor. Because the IFR is a breeder reactor (making more fuel then it uses) it provides an extended supply of uranium and produces no Greenhouse effect. It is deemed to be much safer than oxide fuel reactors and the lifetime of the nuclear waste is dramatically lowered because the long half-life fractions (actinides) are cycled back into the fuel. On-site fuel fabrication and reprocessing makes for a more proliferation resistant operation.

The IFR fuel cycle involves initial fabrication of U-Zr alloy fuel as the initial feed stock, followed by in-reactor ^{235}U burnup resulting in the production of fission products and ^{239}Pu. Subsequently reprocessed (to remove fission products) material, therefore, consists of U-Pu-Zr ternary alloys with gradually increasing Pu content. The maximum stable composition is not yet determined[2].

Under normal operating conditions in the reactor, the fuels are exposed to approximately 150°C radial temperature gradients, with peak fuel centerline

DISCLAIMER

temperatures upwards of 650°C and temperatures along the circumference at approximately 500°C. Ternary phase diagrams show a diversity of phase mixtures in this temperature range, and macroscopic diffusion of Pu and/or Zr along the gradient can be anticipated depending on solubilities of Pu and Zr in the various equilibrium phases. Our experiments probe the fuels over this same temperature range, but in a gradient-free state where the temperature is constant across the fuel. By quantifying the phases present at each temperature, both in relative amounts and chemical composition, we can add valuable data to our current understanding of possible diffusion mechanisms and other stability-related physical parameters.

DIFFRACTION EXPERIMENT

The cylindrical fuel pins used were as-cast material with approximate dimensions 0.223" diameter and 2" length. The three compositions studied are as given in the abstract. All uranium was isotopically depleted (pure ^{238}U, a weak absorber of neutrons) and the plutonium was in the form ^{239}Pu (a relatively high absorber; estimated penetration 1 mm). All samples were doubly welded within thin walled vanadium sleeves *in vacuo*, and for safety reasons the plutonium-containing ones were first placed in quartz sleeves to eliminate contact between Pu and V (see Figure 1).

Neutrons were chosen over X-rays for a number of reasons, the major one being the effect of absorption. Most elements are virtually invisible to neutrons to depths of many inches, allowing bulk sampling. With X-rays, on the other hand, non-destructive bulk sampling of heavy metal fuels is impossible. Oxidation of the sample and vanadium sleeves was prevented by evacuating the sleeves and operating the furnace in a vacuum. This was very readily done for the neutron diffraction experiment where containers and window materials can be metallic.

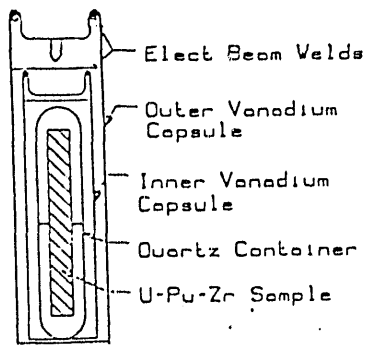

Figure 1. Fuel pins as welded within two concentric thin walled vanadium 0.005" sleeves. An additional quartz sleeve was used for all plutonium-containing pins.

All diffraction data were taken on the GPPD Time-of-Flight powder diffractometer[3] at IPNS, which accepts pulsed neutrons, uses fixed angle detector positions and TOF data collection. Data were analyzed using the Rietveld profile refinement technique[4], modified for time-of-flight diffraction data[5-7].

All patterns were obtained with the samples positioned in a furnace specially designed and constructed by Vaninetti et al.[8] for this type of experiment at IPNS and previously used by them. The basic furnace (shown in Figure 2) consists of two large flat plate resistance heaters, each 7" square, positioned above and below the sample 4" apart, with a suitable hole in the center for insertion of the sample. Two thin vanadium reflection shields surround the sample - one 4" in diameter, sitting on the bottom heater block and the other 7" in diameter held in position with two cylindrical bands. Four thermocouples (chromel-alumel) are attached with wire wrap - 2 near each end of the V capsules. Temperature setting and control are achieved with two Omega controllers using power supplied through two hand-adjusted variacs, one for each heater. Due to a difference in heat dissipation between the two, the variacs were generally set to different values - for example, to achieve 650°C at both ends of the sample with all 4 TC's reading within ±1°C, settings of 110V and 75V top and bottom, respectively, were required. A more sophisticated controlling system for automatic temperature setting, control and changing could be installed if desired. The furnace in its present form has a maximum temperature near 750°C. Temperature gradients across the sample are minimized by the large furnace volume relative to sample size. Full access to the ±150° and ±90° detector banks is achieved by appropriate positioning of support material.

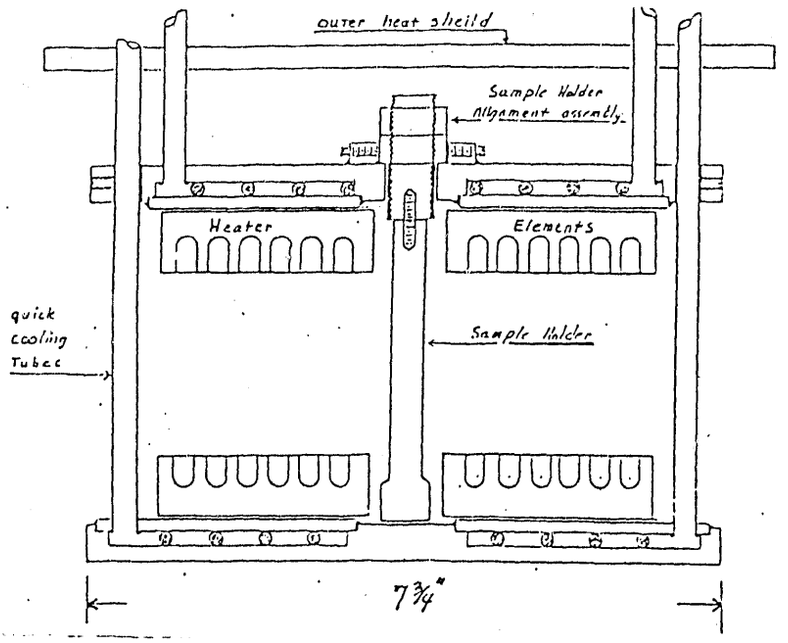

Figure 2. Resistance heater furnace designed by Vaninetti et al. as used (in vacuum) on the GPPD. Double vanadium heat shields not shown.

RESULTS

All results presented here come directly from the Rietveld refinements. Multiple phase refinements were carried out using, for each phase, an asymmetric unit of atomic positions, an asymmetric number of symmetry operations, standard atomic scattering lengths, and occupation factors appropriate to each type of atomic site. Scale factors derived from these refinements, therefore, can be transformed to mole fractions (MF_p) in a manner similar to that spelled out by Hill and Howard[9]:

$$MF_p = S_p(V_pO_pN_p)^2/(Z_p)^2 \,/\, \Sigma_i\, S_i(V_iO_iN_i)^2/(Z_i)^2$$

where S, V, O, N and Z are, respectively, Rietveld scale factor, unit cell volume, number of symmetry operations, occupation factor and number of formula units per unit cell. This analysis is amenable to any number of phases, limited only by our ability to distinguish one phase from another. Thus, detailed interpretation of diffraction peak intensities gives us relative amounts of each of the phases present. We can gain further chemical composition information from the peak positions, i.e., lattice parameters. Solubility of Zr or Pu in α-U, for instance, dramatically expands the α-U parameters. Also, the bcc forms of Zr and U, β-Zr and γ-U, respectively, have significantly different lattice parameters. As a result, in the U/Zr alloy the chemical composition of any co-existing equilibrium bcc solid solution can be inferred from its lattice parameter.

Any alloy containing α-U will be susceptible to anisotropic growth due to preferential orientation of α-U grains. The direction (axial vs. radial) of greatest potential growth can be estimated by measuring the relative intensities of select α-U reflections representing specific crystallographic directions. Evidence for preferred orientation will be provided by the Rietveld refinement in the form of residual intensities greater or less than zero depending on the orientations of the grains relative to the horizontal diffraction plane.

Binary phase diagrams are available for the U-Zr[10], U-Pu[11] and Zr-O[12] systems as are a series of ternary U-Pu-Zr[13] diagrams at selected temperatures ranging from 500°C to 770°C. References 10 and 12 also contain lattice parameter data that are of interest. From these primary sources we have phasal and chemical compositional

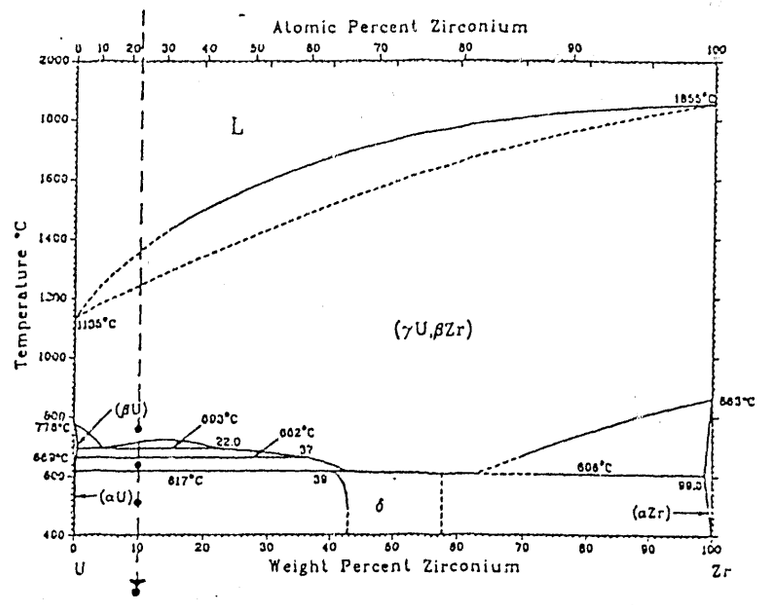

Figure 3. U-Zr phase diagram as given by Sheldon and Peterson together with temperatures indicated at which data were taken.

expectations for each alloy at all temperatures, which can be directly compared with our results.

U-10%Zr

The U-Zr binary phase diagram is given in Figure 3. Our composition (U-10wt.%Zr, U-22 at.%Zr) is identified on the figure (as a vertical line), as are the experimental data points at 25°C, 500°C, 635°C and 750°C. As shown in Table 1, we find from the Rietveld analysis that the expected phases exist at each temperature. Room temperature Based on the very limited expected solubility of Zr in α-U (~0.5%), respective mole fractions of α and δ should be 67% α-U, 33% δ-U/Zr. Our observed

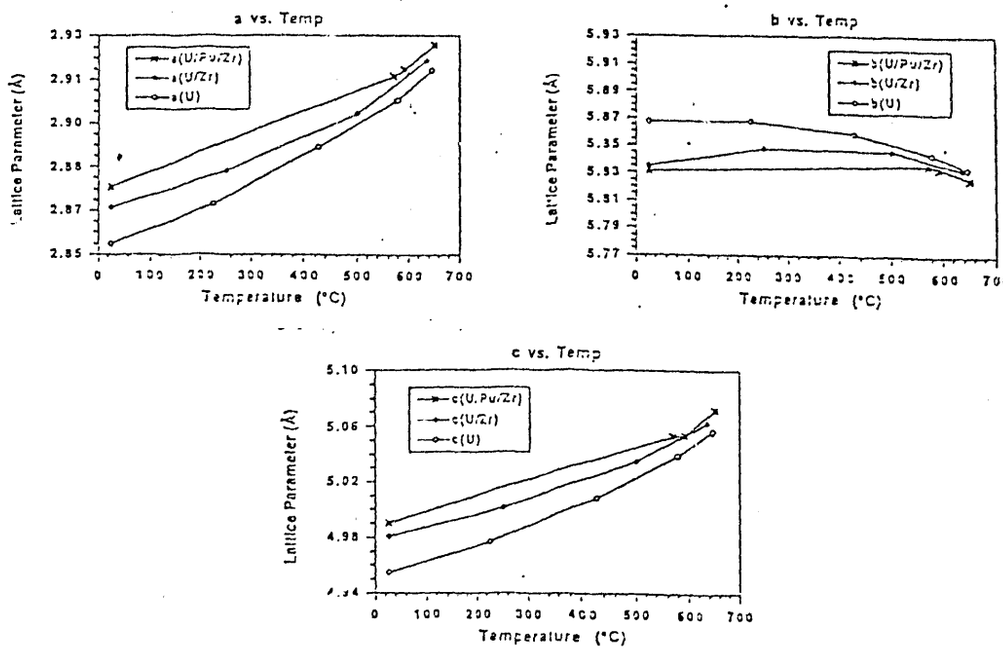

Figure 4. α-U lattice parameters vs. temperature for the two alloy fuel pins (U-Zr and U-Pu-Zr) as compared with pure α-U.

values of 88% and 11% indicate supersaturation of the α-U. Indeed the as-cast alloy is reported[2] to consist primarily of supersaturated α-U, given the designation α'-U. The observed mole fractions (Table 1) are consistent with 15.6% Zr in α'-U. Figure 4 shows the effect on the α-U lattice parameters relative to pure uranium. At room temperature the effect is a 0.5% expansion of a_0 and c_0 and 0.5% contraction of b_0. This effect is approximately the same as raising the temperature of pure U. Unfortunately, no previous data indicating lattice expansion due to solubility of Zr in U exist for comparison. Figure 5

Table 1. Composition (mole percent) vs. temperature for U-10%Zr fuel pin

Temp.	α	δ	β	γ	ZrO	ZrO_{1-x}
25°C	88 %	11 %	-	-	0.6 %	1.1 %
500	72	26	-	-	0.4	1.5
635	71	-	-	27 %	0.4	1.6
750	-	-	-	99	0.3	1.1

shows the Rietveld profile plot for the RT refinement. The generally good fit proves that our mole fractions and lattice parameters are reasonable. Noticeable discrepancies in the intensities of reflections (133), (042) and (023), all of which have orientations near the [020] crystallographic direction, are indicative of potential radial growth. Two oxygen-containing inclusion phases Zr(O,C,N) and ZrO_{1-x} (x~0.75) were clearly identified from weak, isolated diffraction lines not attributable to any of the U-Zr phases. Whereas an earlier X-ray diffraction study[14] suggested the presence of a ZrO_{1-x} phase with no appreciable change in lattice parameters from hexagonal α-Zr, we observed 0.6% and 0.8% increases in a_0 and c_0, respectively. The existence of these latter two phases at all temperatures shows a lack of complete solution of zirconium in uranium. 500°C Observed mole fractions (Table 1) suggest diffusion of Zr from α'-U to δ-U/Zr (4.3% Zr left in α'-U). Lattice parameters are correspondingly closer to those of pure U. 635°C

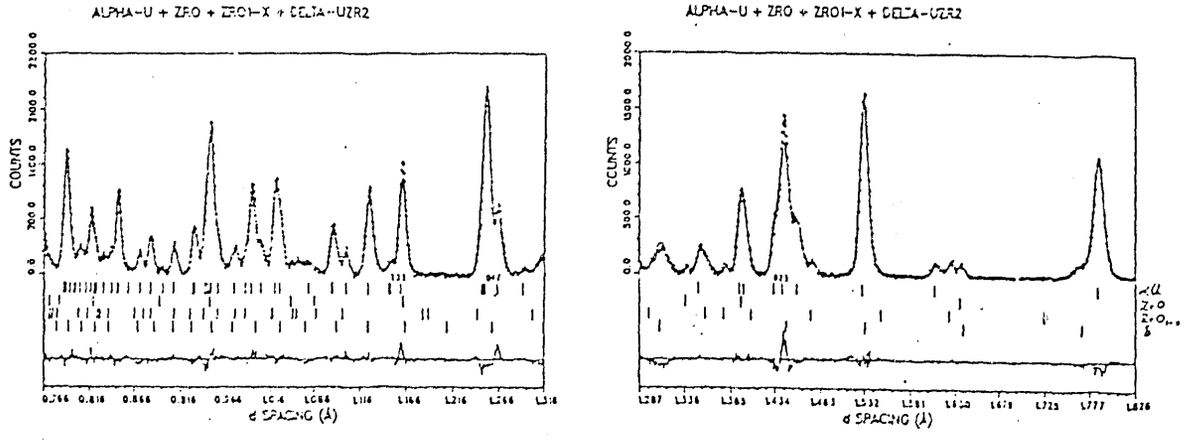

Figure 5. Partial Rietveld plot of U-Zr alloy showing presence of four phases: α'-U, ZrO, ZrO_{1-x} and δ. Residual intensities are shown in the lower plot.

The mole fraction of α'-U remains virtually constant implying that the phase transformation was strictly δ-U/Zr to γ-U/Zr. The lattice parameter of γ-U/Zr (a=3.5822(1) Å) is close to that expected for the composition UZr_2 at this temperature. 750°C This is a single phase region, with lattice parameter (a=3.5542(1) Å) consistent with the known overall composition of the fuel pin.

From these results we conclude that the δ-U/Zr phase has composition UZr_2 and that supersaturation of the α-U phase, caused by fast cooling during fabrication, is reduced as the temperature is raised. Slight preferred orientation of the α'-U phase suggests possible radial growth during heat cycling or irradiation.

U-8%Pu-10%Zr

Representative ternary phase diagrams at 580°C and 660°C are given in Figure 6. These show a complex variation of phase mixtures with composition. For each of the

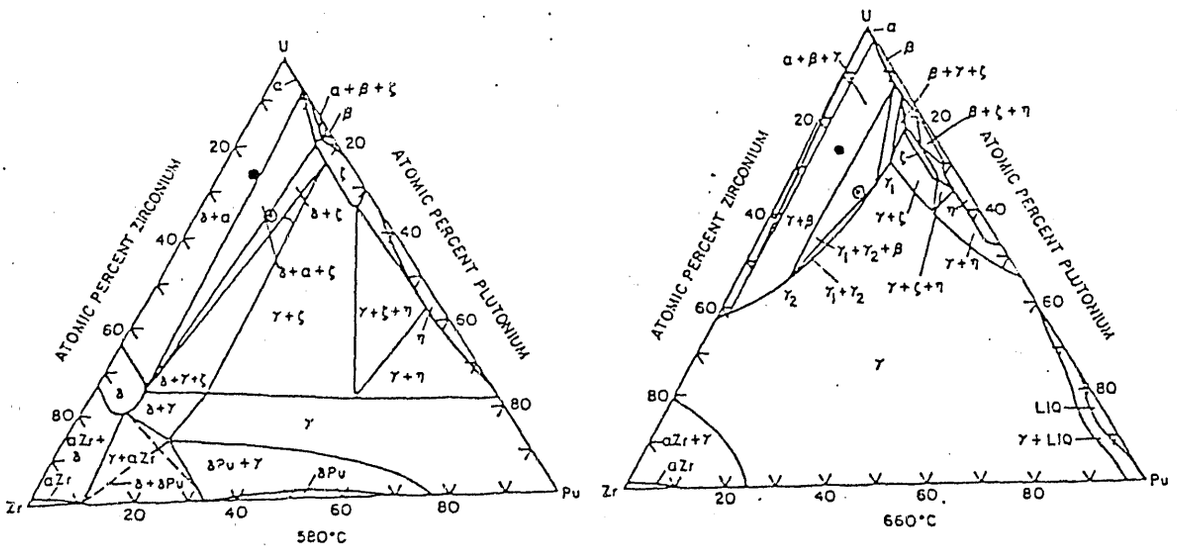

Figure 6. Ternary phase diagram showing location of U-8%Pu-10%Zr (•) and U-19%Pu-10%Zr (o) at 580°C and 660°C.

temperatures we studied, a list of expected phases based on the published phase diagram could be compiled. In most cases this agreed with what was observed, with a couple exceptions. Figure 7a shows portions of raw diffraction data at each of the temperatures indicating the differentiability of all of the phases. Table 2 gives a mole fraction breakdown at each temperature. Room temperature The presence of the 8%Pu does not

Table 2. Composition (mole percent) vs. temperature for U-8%Pu-10%Zr fuel pin

Temp.	α	δ	β	γ	ZrO	ZrO_{1-x}
25°C	80 %	20 %	-	-	-	-
570	71	29	-	-	-	-
590	12	22	66 %	-	-	-
650	3	-	77	20 %	-	-
50	78	22	-	-	-	-

dramatically effect the room temperature phase mixture when compared to what was previously observed in the U-Zr alloy. This is as expected. In fact, relative amounts of α and δ are very similar with more δ in the U-Pu-Zr alloy indicating lower solubility of Zr in α'-U, estimated for U-Pu-Zr at 11.2%. The fact that the peaks are very broad can be expected since the pin was "as cast", i.e., no anneal. The effect of Zr and Pu solubility on α'-U lattice parameters is shown in Figure 4. Even though we suspect less Zr in the α'-U, the effect of Pu on the lattice is expected to be the same; that is the Pu will also expand the a_0 and c_0 and shrink the b_0. 570°C At this elevated temperature the pattern is considerably sharper (due to the annealing effect). The dominant phases are still α and

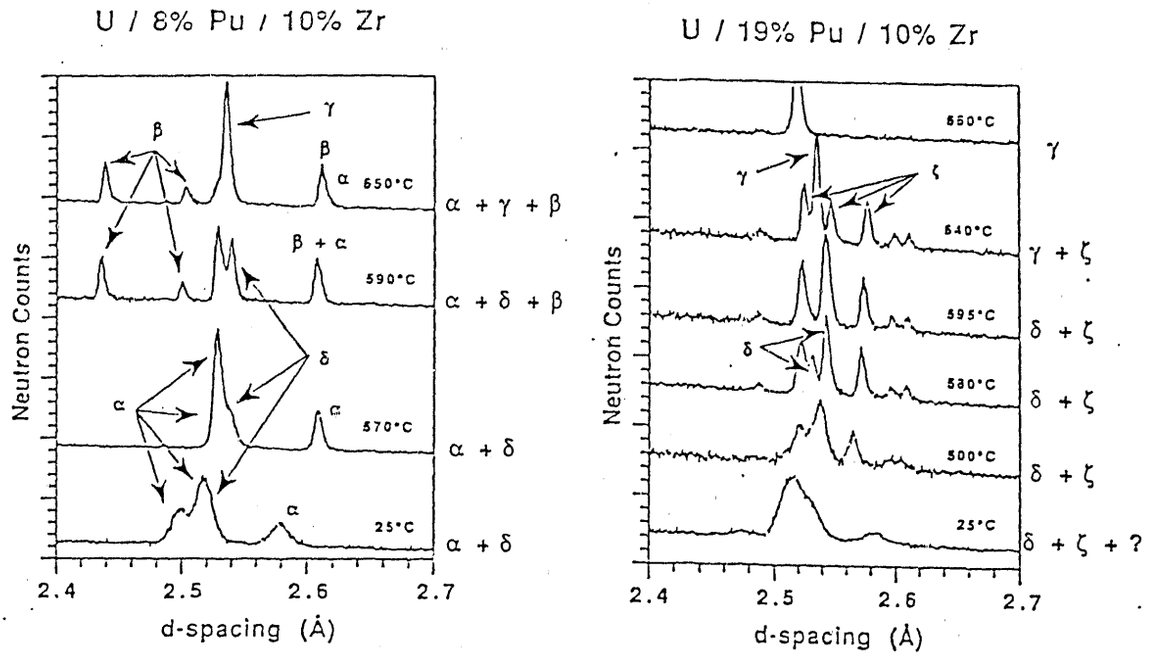

Figure 7. Sections of raw diffraction data for (a) U-8%Pu-10%Zr and (b) U-19%Pu-10%Zr alloys showing phases present in temperature range 25-660°C.

δ. As shown in Table 2, the amount of α has decreased slightly with a corresponding increase in the amount of δ, again indicating decreased solubility of Zr in U (estimated at 4.2%). 590°C At this temperature, the phase diagram suggests the coexistence of α, γ, δ and/or ζ. According to our data there is clearly some δ remaining and probably not γ. This is somewhat difficult to determine with certainty, since the γ unit cell is actually a subcell of the δ cell. From Table 2 it would appear that, in heating from 570°C to 590°C, a large portion of α has transformed to β (not anticipated in the phase diagrams) together

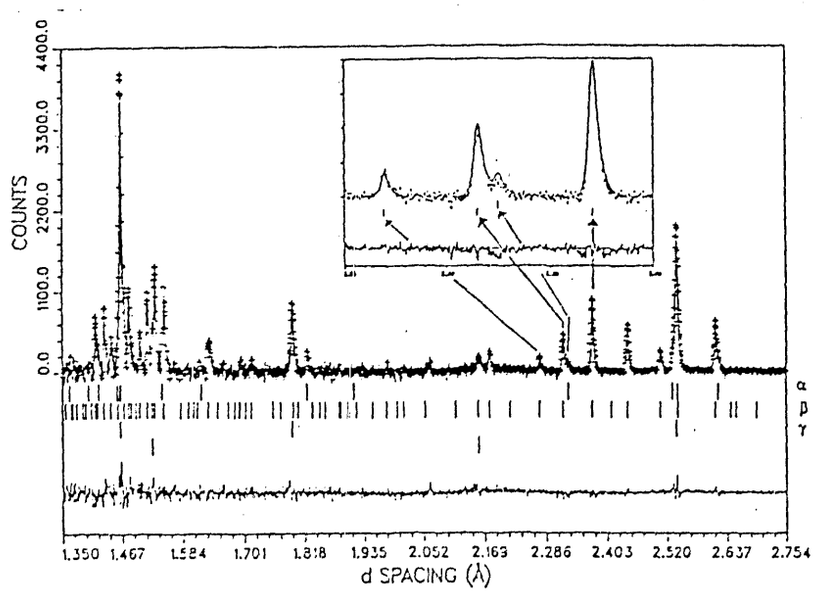

Figure 8. Partial Rietveld profile plot of U-8%Pu-10%Zr alloy at 650°C showing presence of α, β and γ phases. Insert is expanded section specifically showing the presence of the α phase.

with some δ also going to β. The β pattern is a well-known complex pattern which is easy to recognize. 650°C At this temperature, δ is transformed to γ and the transformation of α to β is nearly complete. The transformation of δ to γ and vise versa is quite unique, involving the formation of a small hexagonal (δ) unit cell from a 3x3x3 stacking of the basic γ-cell. The following relationships exist between the orientations of the two cells: γ-[111] equivalent to δ-[001] and γ-[110] to δ-[100]. Essentially all of the γ phase developed during the heating from 590°C to 650°C appears to come from δ; the two phases exist in approximately equal amounts at the two different temperatures and the lattice parameter (a_0=3.5836(1) Å) for γ at 650°C is consistent with composition UZr_2. Figure 8 is a partial Rietveld profile plot from the 650°C refinement showing the evidence for the α, β and γ phases. Even though the amount of α is very small (2-3%), the blow-up of a section of the data in the insert in Figure 8 gives unique evidence for its presence.

U-19%Pu-10%Zr

The patterns obtained from this alloy, given in Figure 7b, show a much different behavior from the other two alloys. Our analysis of these patterns has only just begun, but a few observations can be made: (1) the pattern at 25°C is very broad (casting strains again) but sharpens considerably at 500°C showing the presence of the δ phase and extra lines which become more clearly delineated at 580°C and 595°C as a new phase (probably ζ). Then at 640°C we observe the transformation of δ to γ plus the retention of this new phase. Finally, at 660°C we have strictly γ with lattice parameter a_0=3.5602(2) Å. We are well aware that there is a large contribution to the background from the quartz capsule surrounding the Pu alloy pins for both the 8%Pu and 19%Pu alloys. In Figure 9, we show the magnitude of this contribution in the U-19%Pu-10%Zr sample and how effectively it is removed via Fourier-filtering[15].

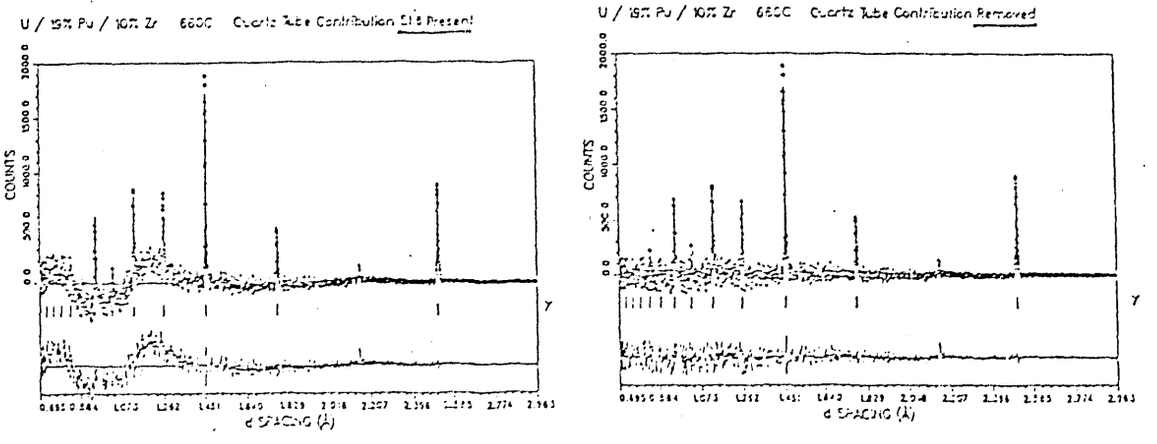

Figure 9. Rietveld profile plot of the U-19%Pu-10%Zr alloy showing the contribution from the quartz tube which surrounds the sample before and after Fourier-filtering.

CONCLUSION

We are quite pleased with the data (available only with the use of neutrons which are able to penetrate into samples with relatively high ^{239}Pu - a highly absorbing material - content) and encouraged by the encapsulating procedure in which the alloy pins are contained in double welded, thin-walled vanadium tubing; with the pin itself surrounded with a quartz capsule. The sizable amorphous pattern which results was removed by Fourier-filtering. We are indeed excited about the phase characterization opportunities with this complex mixture using the Rietveld profile refinement technique. Currently we

have the ability to analyze up to 4 crystalline phases simultaneously; if need be this could be expanded. The U-Pu-Zr ternary system is quite complex as shown in Tables 1 and 2 and Figure 8 and 9. It is important to recognize that reprocessing of the fuel to higher and higher Pu contents does not have a strictly continuous effect on the phase composition. There are discontinuities involved at specific compositions which may be different at each temperature.

ACKNOWLEDGEMENTS

We wish to acknowledge the help of Richard L. Hitterman in carrying out these experiments, thanks to Henry Thresh, Jim Summers and their group for preparing the samples and to the IPNS Support Staff for their assistance during the course of the data collection. This manuscript has been authored by contractors of the U.S. Government under contract W-31-109-ENG-38.

REFERENCES

1. Till, C.E. and Chang, Y.I. *Proc. Amer. Power Conf.* 1989, **51**, 688-691.

2. Hofman, G.L., Pahl, R.G., Lahm, C.E. and Porter, D.L. *Met. Trans A.* 1990, **21A**, 517.

3. Jorgensen, J.D., Faber, Jr., J., Carpenter, J.M., Crawford, R.K., Haumann, J.R., Hitterman, R.L., Kleb, R., Ostrowski, G.E., Rotella, F.J. and Worlton, T.G. *J. Appl. Cryst.* 1989, **22**, 321

4. Rietveld, H.M. *J. Appl. Cryst.* 1969, **2**, 65-71.

5. Von Dreele, R.B.; Jorgensen, J.D. and Windsor, C.G. *J. Appl. Cryst.* 1982, **15**, 581-589.

6. Jorgensen, J.D. and Rotella, F.J. *J. Appl. Cryst.* 1982, **15**, 27-34.

7. Rotella, F.J. Users Manual for Rietveld Analysis of Time-of-Flight Neutron Powder Diffraction Data at IPNS, Argonne National Laboratory, USA, 1986.

8. Vaninetti, J., Lawson, A. C. and Goldstone, J. A., private communication.

9. Hill, R.J. and Howard, C.J. *J. Appl. Cryst.* 1987, **20**, 467-474.

10. Sheldon, R.I. and Peterson, D.E. *Bull. Alloy Phase Diag.* 1989, **10(2)**, 165-171.

11. Peterson, D.E. and Foltyn, E.M. *Bull. Alloy Phase Diag.* 1989, **10(2)**, 160-164.

12. Abriata, J.P., Garces, J. and Versaci, R. *Bull. Alloy Phase Diag.* 1986, **7(2)**, 116-124.

13. O'Boyle, D.R. and Dwight, A.E. "Plutonium 1970 and Other Actinides", *Proc. of 4th Int. Conf. on Pu and Other Actinides* 1970, 720-733.

14. Wonnell, T.J. M.S. Thesis, University of California (Berkeley), Aug. 1988.

15. Richardson, Jr., J.W. and Faber, Jr., J. *Adv. X-ray Anal.* 1986, **29**,143-152.

END

DATE FILMED

12/26/90